

Investigating *lasp-2* in cell adhesion: new binding partners and roles in motility

Katherine T. Bliss, Miensheng Chu, Colin M. Jones-Weinert, and Carol C. Gregorio

Department of Cellular and Molecular Medicine and Sarver Molecular Cardiovascular Research Program, University of Arizona, Tucson, AZ 85724

ABSTRACT Focal adhesions are intricate protein complexes that facilitate cell attachment, migration, and cellular communication. *Lasp-2* (LIM-nebulette), a member of the nebulin family of actin-binding proteins, is a newly identified component of these complexes. To gain further insights into the functional role of *lasp-2*, we identified two additional binding partners of *lasp-2*: the integral focal adhesion proteins vinculin and paxillin. Of interest, the interaction of *lasp-2* with its binding partners vinculin and paxillin is significantly reduced in the presence of *lasp-1*, another nebulin family member. The presence of *lasp-2* appears to enhance the interaction of vinculin and paxillin with each other; however, as with the interaction of *lasp-2* with vinculin or paxillin, this effect is greatly diminished in the presence of excess *lasp-1*. This suggests that the interplay between *lasp-2* and *lasp-1* could be an adhesion regulatory mechanism. *Lasp-2*'s potential role in metastasis is revealed, as overexpression of *lasp-2* in either SW620 or PC-3B1 cells—metastatic cancer cell lines—increases cell migration but impedes cell invasion, suggesting that the enhanced interaction of vinculin and paxillin may functionally destabilize focal adhesion composition. Taken together, these data suggest that *lasp-2* has an important role in coordinating and regulating the composition and dynamics of focal adhesions.

Monitoring Editor

Yu-Li Wang
Carnegie Mellon University

Received: Oct 9, 2012

Revised: Jan 22, 2013

Accepted: Jan 31, 2013

INTRODUCTION

Focal adhesions are protein-dense regions that occupy extracellular, transmembrane, and cytoplasmic compartments of the cell. These complex protein assemblies make contact with the extracellular matrix and facilitate cell attachment, migration, and cellular communication. The number of focal adhesion proteins identified is growing and comprises a mixture of cytoskeletal and signaling proteins (for reviews see Wozniak *et al.*, 2004; Lo, 2006). Focal adhesions display an extremely well-organized molecular composition with layers of distinct protein–protein interactions (Kanchanawong *et al.*, 2010).

Although focal adhesions might appear to be relatively static structures, many components cycle in and out at different rates depending on the activation and posttranslational modifications of several key proteins (e.g., Humphries *et al.*, 2007; Deramautd *et al.*, 2011). In fact, it is the dynamics and turnover of new focal adhesions forming at the leading edge of the cell and older focal adhesions disassembling that are important contributors for cell spreading and migration (for reviews see Le Clairche and Carlier, 2008; Gardel *et al.*, 2010). Although cell migration and spreading is required for normal biological processes, aberrant regulation of the adhesion and cytoskeletal machinery is the fundamental mechanism of cancer cell metastasis and invasion.

Adding to the list of focal adhesion components is *lasp-2* (LIM-nebulette), a member of the nebulin family of actin-binding proteins (Katoh, 2003; Li *et al.*, 2004; Terasaki *et al.*, 2004). Proteins in the nebulin family contain differing numbers of the characteristic “nebulin repeat,” which is an ~35-residue repeat containing an actin-binding SDxxYK motif (Labeit *et al.*, 1991). *Lasp-2* is a splice variant of the cardiac-specific nebulin family member nebulette (Moncman and Wang, 1995; Katoh, 2003). Although it is an isoform of nebulette, *lasp-2* differs significantly in its modular domain organization since it has four unique exons and is also likely transcribed from a promoter that is not specific to striated muscle (Li *et al.*, 2004). The

This article was published online ahead of print in MBoc in Press (<http://www.molbiolcell.org/cgi/doi/10.1091/mbc.E12-10-0723>) on February 6, 2013.

Address correspondence to: Carol C. Gregorio (gregorio@email.arizona.edu).

Abbreviations used: Co-IP, coimmunoprecipitation; ELISA, enzyme-linked immunosorbent assay; F-actin, filamentous actin; FBS, fetal bovine serum; GAPDH, glyceraldehyde 3-phosphate dehydrogenase; GFP, green fluorescent protein; GST, glutathione S-transferase; HEK 293, human embryonic kidney 293 cells; His, histidine; PBS, phosphate-buffered saline; SH3, SRC homology 3 domain; siRNA, small interfering RNA; Y2H, yeast two-hybrid.

© 2013 Bliss *et al.* This article is distributed by The American Society for Cell Biology under license from the author(s). Two months after publication it is available to the public under an Attribution–Noncommercial–Share Alike 3.0 Unported Creative Commons License (<http://creativecommons.org/licenses/by-nc-sa/3.0>).

“ASCB®,” “The American Society for Cell Biology®,” and “Molecular Biology of the Cell®” are registered trademarks of The American Society of Cell Biology.

tissue expression profile of *lasp-2* includes abundant protein levels in the brain but also expression in the lung, kidney, and striated muscle (Li *et al.*, 2004; Terasaki *et al.*, 2004; Zieseniss *et al.*, 2008). *Lasp-2* exhibits a high degree of homology to another nebulin family member, *lasp-1* (Tomasetto *et al.*, 1995), although these proteins are transcribed from separate genes (Katoh, 2003). Both *lasp-2* and *lasp-1* contain an N-terminal LIM domain, either three nebulin repeats (*lasp-2*) or two nebulin repeats (*lasp-1*), and a C-terminal SH3 domain (Schreiber *et al.*, 1998; Terasaki *et al.*, 2006). *Lasp-1* is ubiquitously expressed and, like *lasp-2*, is a component of focal adhesions and binds zyxin and F-actin (Chew *et al.*, 2002; Li *et al.*, 2004). Changes in protein levels of *lasp-1* have been shown to have effects on cell migration, focal adhesion dynamics, and proliferation (Lin *et al.*, 2004; Grunewald *et al.*, 2006, 2007; Zhang *et al.*, 2009). Increased *lasp-1* protein expression is also found in tumors associated with metastatic ovarian, breast, and colorectal cancer (Tomasetto *et al.*, 1995; Grunewald *et al.*, 2006, 2007; Zhao *et al.*, 2010). Although *lasp-1*'s link to metastasis is significant, it is notable that *lasp-2*'s potential role in this phenomenon has not yet been examined.

Lasp-2 is reported to localize in focal adhesions and actin filament bundles, based on the assembly patterns of GFP-*lasp-2* in several cell lines (HeLa, NIH3T3, PtK2, C2C12, and NG108-15; Li *et al.*, 2004; Terasaki *et al.*, 2004; Panaviene and Moncman, 2007; Deng *et al.*, 2008; Nakagawa *et al.*, 2009). In striated muscle, green fluorescent protein (GFP)-*lasp-2* also localizes to focal adhesions, as well as to Z-disks and intercalated disks of cardiomyocytes (Panaviene and Moncman, 2007; Zieseniss *et al.*, 2008). *Lasp-2* can bind and bundle actin filaments, and the addition of α -actinin, a *lasp-2* binding partner, results in thicker, more robust actin filament bundles (Zieseniss *et al.*, 2008).

Recently attention has focused on the role of *lasp-2* in focal adhesion function and organization. Not only does *lasp-2* bind F-actin and α -actinin (both found at focal adhesions), but it also binds the focal adhesion protein zyxin (Li *et al.*, 2004). Zyxin is an integral focal adhesion molecule with roles in actin organization, stress fiber repair, assembly, and cell motility (e.g., Crawford and Beckerle, 1991; Hirata *et al.*, 2008; Smith *et al.*, 2010; for review see Beckerle, 1997). Zyxin also has the ability to shuttle to the nucleus, where it can interact with transcription factors (Wang and Gilmore, 2003; Hervy *et al.*, 2006). *Lasp-2*, through its localization to focal adhesions, interacts with the actin cytoskeleton and, presumably with the cooperation of some of its binding partners, appears to play a role in cell spreading (Deng *et al.*, 2008). Although the localization of *lasp-2* to focal adhesions is established, little is known about the functional role of *lasp-2* in these structures, its relationship with other focal adhesion proteins, and its function in cell motility.

To provide further insights into the functional role(s) of *lasp-2* in actin dynamics and at focal adhesions, we first sought to identify novel *lasp-2* binding partners. Two focal adhesion/actin-associated proteins, vinculin and paxillin, were identified as *lasp-2* binding partners. The SH3 domain of *lasp-2* was mapped as the binding site for both vinculin and paxillin. Of interest, it is the LIM domain and nebulin repeats (and not the SH3 domain) of *lasp-2* that are required for the localization of *lasp-2* to both focal adhesions and the cortical actin cytoskeleton. Functionally altering the levels of *lasp-2* in metastatic cancer cells (SW620 or PC-3B1) results in enhanced cell migration, indicating that *lasp-2* has a critical role in the regulation of focal adhesion dynamics. Taken together, our data support the hypothesis that *lasp-2* is an important scaffold for several key focal adhesion proteins and has a pivotal role in regulating the composition and dynamics of these cytoskeletal assemblies.

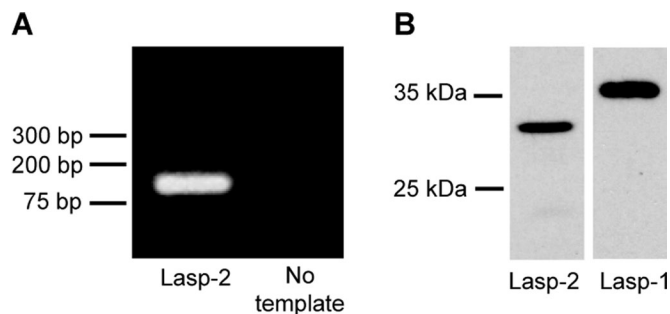


FIGURE 1: *Lasp-2* is expressed in HEK 293 cells. RT-PCR analysis detects *lasp-2* transcript in HEK 293 cells. (A) *Lasp-2*-specific primers amplify a single band of the expected size. (B) HEK 293 cell protein lysates were analyzed by Western blot analysis. Our anti-*Lasp-2*-specific antibody recognizes a single protein band migrating slightly below 35 kDa, whereas an anti-*lasp-1* antibody detects a protein band above 35 kDa.

RESULTS

Lasp-2 interacts with the focal adhesion proteins vinculin and paxillin

To probe for the functional role of *lasp-2* in mammalian cells, we used human embryonic kidney cells (HEK 293) because reverse transcription (RT)-PCR with *lasp-2*-specific primers showed that HEK 293 cells express *lasp-2* transcripts (Figure 1A). To specifically detect *lasp-2*, we generated monoclonal antibodies against the C-terminus of *lasp-2* and chose a clone that does not recognize *lasp-1* in our assays. The reactivity of the antibody to *lasp-2* and not to *lasp-1* or other cellular proteins was determined by probing Western blots of cell lysates expressing recombinant *lasp-1*. This is important because all anti-*lasp-2* antibodies that are available appear to have the potential to bind *lasp-1* (e.g., Supplemental Figure S1). Western blot analysis with our monoclonal anti-*lasp-2* antibody shows that *lasp-2* is detected in HEK 293 cells (Figure 1B). Because our monoclonal anti-*lasp-2*-specific antibodies do not work by immunofluorescence microscopy, in order to visualize *lasp-2*, we transfected HEK 293 cells with GFP-*lasp-2* and evaluated them by immunofluorescence microscopy. *Lasp-2* localizes to focal adhesion plaques, as indicated by colocalization with the known focal adhesion protein vinculin (Figure 2A). This localization to focal adhesions is consistent with other studies (Li *et al.*, 2004; Deng *et al.*, 2008; Nakagawa *et al.*, 2009).

Because we hypothesize that *lasp-2* has a role as a molecular scaffold, we next sought to identify other components that interact with *Lasp-2* in these structures. We used a candidate yeast two-hybrid approach. Vinculin, an important structural focal adhesion component, was chosen as a candidate because it colocalizes with *lasp-2* (Figure 2A) and contains a proline-rich region that might be a target for the SH3 domain of *lasp-2*. Vinculin is composed of a globular head domain and a tail domain (which includes a short, 40-amino acid, proline-rich neck region). Prey constructs containing full-length as well as the head and tail domains were generated. Initially, full-length *lasp-2* was expressed as bait and cotransformed into yeast strain AH109 with full-length vinculin as prey. *Lasp-2* was found to interact with vinculin. The tail domain of vinculin but not the head domain interacted with *lasp-2* in this assay (Figure 2B). In addition, by using *lasp-2* truncations in this assay, we found the binding site for vinculin to be the SH3 domain of *lasp-2* (Figure 2C). Proline-rich regions are well-described binding sites for SH3 domains (Yu *et al.*, 1994). Indeed, the proline-rich region of vinculin is contained within

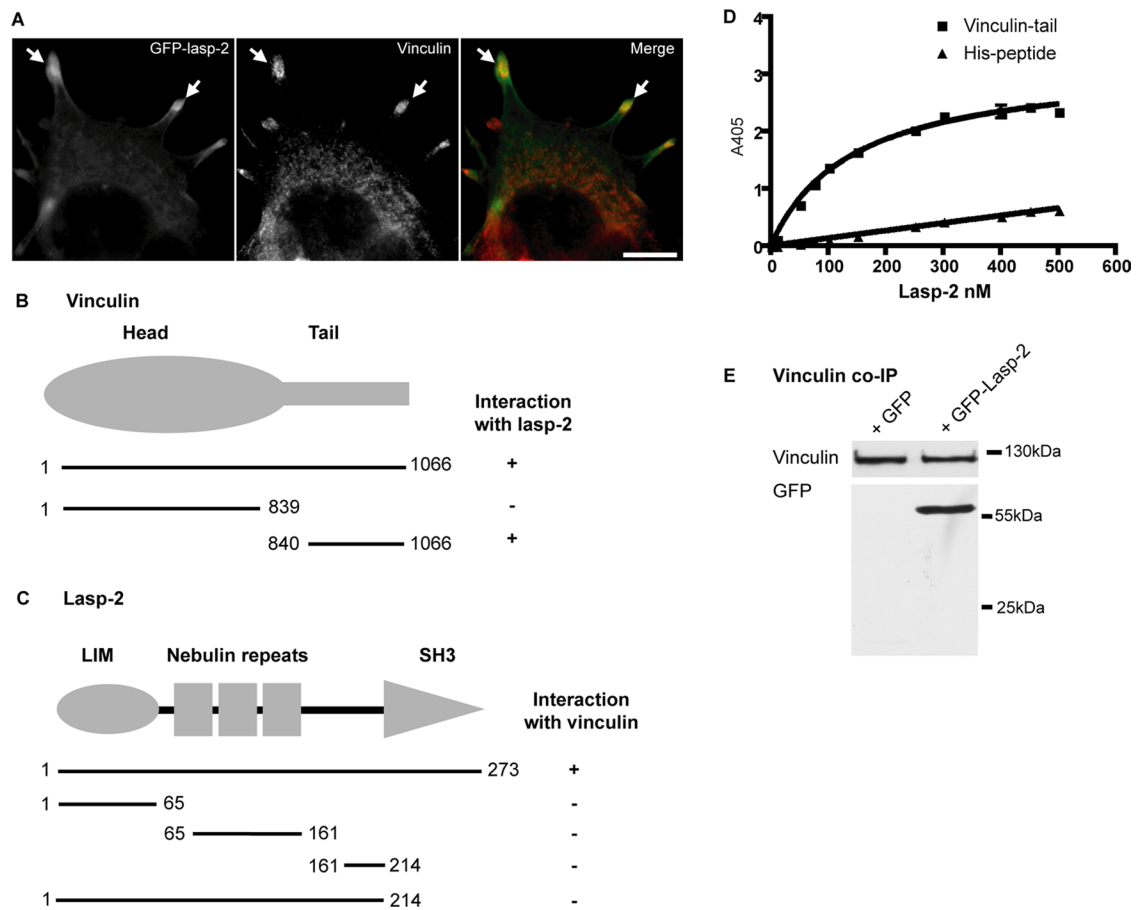


FIGURE 2: Lasp-2 interacts with vinculin. (A) Lasp-2 (green) colocalizes with vinculin (red) at focal adhesions. HEK 293 cells were transfected with GFP-lasp-2 and stained for vinculin. Areas of colocalization are highlighted with arrows. Scale bar, 10 μ m. (B) For analysis with the yeast two-hybrid (Y2H) system, yeast strain AH109 was cotransfected with a bait coding for lasp-2 and a prey coding for vinculin. Various vinculin prey fragments were then cotransformed with lasp-2, and the binding site for lasp-2 on vinculin was determined to be within the vinculin-tail. (C) Also using the Y2H system, the binding site for vinculin on lasp-2 was found to be the SH3 domain of lasp-2 using different lasp-2 bait constructs. (D) Lasp-2 binds to vinculin-tail in a saturable manner in ELISA. A 10-pmol amount of vinculin-tail or His-peptide (negative control) was immobilized on microtiter plates and incubated with increasing amounts of lasp-2. Bound lasp-2 was detected with an anti-lasp-2 antibody. Lasp-2 bound to vinculin-tail but much less to His-peptide. (E) Lasp-2 coimmunoprecipitates with vinculin. Endogenous vinculin was immunoprecipitated from HEK 293 cell lysates expressing either GFP or GFP-lasp-2. GFP-lasp-2 coimmunoprecipitated with vinculin.

the tail/neck domain construct, and so it is likely the target for the SH3 domain of lasp-2.

To confirm the interaction of lasp-2 with vinculin, solid-phase binding assays (enzyme-linked immunosorbent assays [ELISAs]) were performed. Purified recombinant vinculin-tail was absorbed onto microtiter plates and incubated with increasing amounts of recombinant lasp-2. The amount of bound lasp-2 was detected using an anti-lasp-2 antibody. Results from these experiments demonstrate that lasp-2 binds to vinculin-tail directly and the binding was saturable, with an approximate K_d of 140 nM (Figure 2D).

To investigate whether lasp-2 and vinculin can form a molecular complex in cells, we performed coimmunoprecipitation experiments. GFP-lasp-2 was expressed in HEK 293 cells. Endogenous vinculin was immunoprecipitated using an anti-vinculin antibody. GFP-lasp-2 was coimmunoprecipitated with vinculin (Figure 2E). The identity of vinculin and GFP-lasp-2 in the complex was verified by Western blot analysis (Figure 2E). In addition, the SH3 domain of lasp-2 is sufficient to interact with vinculin in coimmunoprecipitation experiments (Supplemental Figure S3).

Given our hypothesis that lasp-2 is a scaffolding protein, we also tested whether it interacted with paxillin, another dynamic, focal adhesion component. Paxillin was a likely candidate because it has a very similar domain organization to zyxin (a lasp-2 binding partner). Lasp-2 also colocalizes with endogenous paxillin in HEK 293 cells (Figure 3A). Via a yeast two-hybrid assay with full-length Lasp-2 as bait and full-length paxillin as prey, we detected an interaction. Further analysis showed that lasp-2 lacking the SH3 domain did not interact with paxillin, indicating that the SH3 domain of lasp-2 is likely to be the domain responsible for paxillin binding (Figure 3B). Note that the SH3 domain alone cannot be used in this yeast two-hybrid assay because it autoactivates; thus the direct interaction involving the SH3 domain of lasp-2 could not be tested using this approach.

The direct interaction of lasp-2 with paxillin was confirmed using ELISAs. Purified recombinant glutathione S-transferase (GST)-lasp-2 was absorbed onto microtiter plates and incubated with increasing amounts of recombinant paxillin. Paxillin bound to GST-lasp-2 in a saturable manner, whereas paxillin did not bind to GST alone (Figure 3C). The K_d value for this interaction was \sim 20 nM.

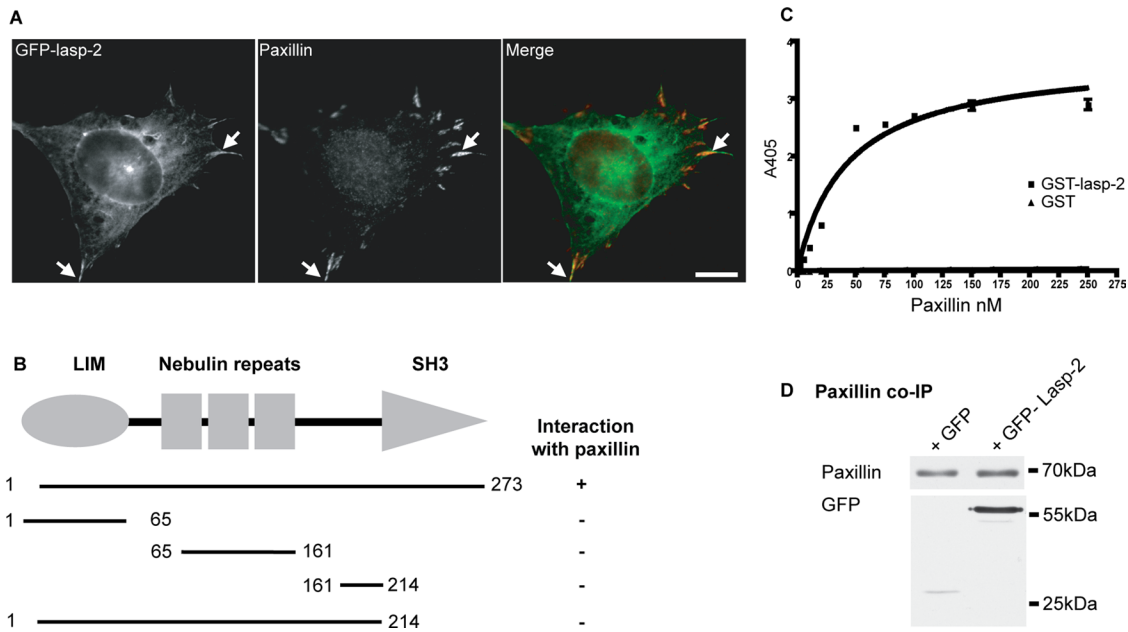


FIGURE 3: Lasp-2 interacts with paxillin. (A) Lasp-2 (green) colocalizes with paxillin (red) at focal adhesions. HEK 293 cells were transfected with GFP-lasp-2 and stained for paxillin. Areas of colocalization are highlighted with arrows. Scale bar, 10 μ m. (B) For analysis with the Y2H, yeast strain AH109 was cotransfected with a bait vector coding for lasp-2 and a prey vector coding for paxillin. The binding site for paxillin on lasp-2 was found to be the SH3 domain of lasp-2 using different lasp-2 bait constructs. (C) Paxillin binds to lasp-2 in a saturable manner in ELISA. A 10-pmol amount of GST-lasp-2 or GST alone was immobilized on microtiter plates and incubated with increasing amounts of paxillin. Bound paxillin was detected with an anti-paxillin antibody. (D) Lasp-2 coimmunoprecipitates with paxillin. Endogenous paxillin was immunoprecipitated from HEK 293 cell lysates expressing either GFP or GFP-lasp-2. GFP-lasp-2 coimmunoprecipitated with paxillin.

To evaluate whether lasp-2 can form a complex with paxillin from cell lysates, we again performed coimmunoprecipitation experiments. GFP-lasp-2 or GFP alone was expressed in HEK 293 cells, and endogenous paxillin was immunoprecipitated using an anti-paxillin antibody. GFP-lasp-2 coimmunoprecipitated with paxillin, whereas GFP alone is nearly undetectable in the precipitate (Figure 3D). Moreover, the SH3 domain of lasp-2, which interacts with vinculin (see earlier discussion), is also sufficient to interact with paxillin in coimmunoprecipitation assays (Supplemental Figure S3). These results indicate not only that lasp-2 is localized to focal adhesions but that it also interacts directly with several important components of focal adhesions—vinculin, paxillin (this study), and zyxin (Li *et al.*, 2004)—and it can do so both directly (yeast two-hybrid; ELISA) and in the context of a cellular environment (coimmunoprecipitation).

Lasp-2 interaction with paxillin and vinculin is reduced in the presence of Lasp-1

As was shown, Lasp-2 will robustly coimmunoprecipitate with vinculin and paxillin. Because lasp-1 is a closely related nebulin family member to lasp-2, we tested whether lasp-1 would also coimmunoprecipitate with vinculin and paxillin. Cherry-lasp-1 was expressed in HEK 293 cells, and endogenous vinculin (Figure 4A) or paxillin (Figure 4B) was immunoprecipitated from these cells. Compared to lasp-2, the amount of lasp-1 that was coimmunoprecipitated with paxillin or vinculin was low and/or undetectable (Figure 4). When lasp-1 is coexpressed along with lasp-2, the amount of lasp-2 that coimmunoprecipitates with endogenous vinculin or paxillin is significantly reduced (Figure 4, A and B). The lack of a detectable interaction between lasp-1 with vinculin and paxillin or the loss of the lasp-2 interaction with vinculin and paxillin in the presence of lasp-1

is not due to a shift of vinculin or paxillin into the insoluble lysate fraction (Supplemental Figure S2).

These results suggest that the binding affinity of lasp-2 for vinculin or paxillin protein complexes is higher than the affinity of lasp-1 for these same complexes. In addition, lasp-1 appears to interfere with the ability of lasp-2 to bind vinculin or paxillin. One possible explanation for how lasp-1 disrupts the binding of lasp-2 with vinculin or paxillin is that lasp-1 itself binds lasp-2. Indeed, yeast two-hybrid assays using lasp-2 as bait and lasp-1 as prey showed a positive interaction (Figure 4C), indicating that the two proteins can interact. The interaction of lasp-1 and lasp-2 was confirmed using a solid-phase binding assay. Histidine (His)-lasp-2 or His peptide alone was absorbed onto microtiter plates and incubated with increasing amounts of GST-lasp-1. GST-lasp-1 interacted with His-lasp-2 in a saturable manner (Figure 4D). The K_D value for this interaction was \sim 15 nM. These data suggest that lasp-1 directly impedes the binding of lasp-2 to vinculin or paxillin.

The interaction of vinculin and paxillin is enhanced in the presence of Lasp-2

Vinculin and paxillin interact with each other (Turner *et al.*, 1990) as well as with lasp-2 (this study). To investigate the effect of lasp-2 on the interaction of vinculin and paxillin, endogenous vinculin was immunoprecipitated in cells expressing GFP-paxillin, GFP-lasp-2, or GFP alone (control). In the presence of GFP-lasp-2, the amount of paxillin pulled down with endogenous vinculin complex was significantly increased (Figure 5). Thus lasp-2 appears to enhance the interaction of vinculin and paxillin, possibly by stabilizing their binding. This enhancement does not appear to be maintained in the presence of lasp-1 (Figure 5).

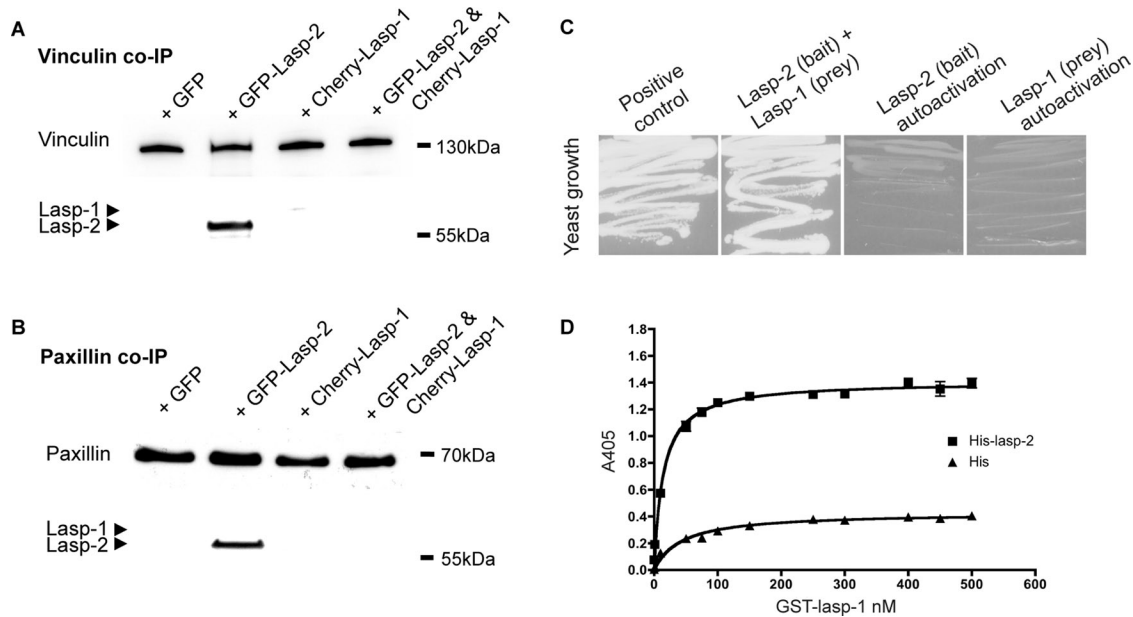


FIGURE 4: The *lasp-2* interaction with paxillin and vinculin is greatly reduced in the presence of *lasp-1*. (A) GFP-*lasp-2* coimmunoprecipitates with endogenous vinculin from HEK 293 cell lysates. Very little, if any, Cherry-*lasp-1* is found to coimmunoprecipitate. However, when GFP-*lasp-2* and Cherry-*lasp-1* are coexpressed in HEK 293 cells, the interaction of GFP-*lasp-2* with vinculin is diminished. (B) Similarly, GFP-*lasp-2* coimmunoprecipitates with endogenous paxillin from HEK 293 cell lysates, whereas Cherry-*lasp-1* is hardly detected. When GFP-*lasp-2* and Cherry-*lasp-1* are coexpressed, the interaction of *lasp-2* with paxillin is nearly undetectable. (C) The potential interaction of *lasp-2* with *lasp-1* was evaluated via yeast two-hybrid analysis. *Lasp-2* as a bait construct interacted with *lasp-1* as a prey construct, as indicated by yeast growth on growth selection plates. (D) The interaction of *lasp-2* with *lasp-1* was confirmed using ELISA. GST-*lasp-1* bound to His-*lasp-2* in a saturable manner.

The LIM-nebulin-linker domain is important for localizing *Lasp-2* in HEK 293 cells

To further determine how *lasp-2* plays a role in focal adhesion composition and to better understand its functional domains, we examined the propensity of *lasp-2* fragments to assemble. HEK 293 cells were transfected with GFP, GFP-*lasp-2*, GFP-*lasp-2* 1–214 (containing the LIM domain, nebulin repeats, and linker) or GFP-*lasp-2* 161–273 (containing the linker and SH3 domain), fixed, and stained for vinculin to mark focal adhesions. As expected, full-length GFP-*lasp-2* localizes to focal adhesions (Figure 6). *Lasp-2* was observed to colocalize with vinculin in some areas, whereas in other areas *lasp-2* assembled without detectable vinculin. Unexpectedly, however, GFP-*lasp-2* 1–214 localized similarly to full-length GFP-*lasp-2*. This was surprising because studies of *lasp-2* in fibroblast cell lines demonstrated that the linker-SH3 domain is necessary for targeting *lasp-2* to focal adhesions (Panaviene and Moncman, 2007; Nakagawa *et al.*, 2009). In contrast, GFP-*lasp-2* 161–273 was not observed to assemble, and in fact its distribution was indistinguishable from the diffuse cytoplasmic and nuclear distribution of GFP alone (Figure 6). The assembly patterns of different *lasp-2* fragments suggest that it is the LIM domain and nebulin repeats, and thus potentially the actin-binding activity of *lasp-2*, that allow for its proper assembly in HEK 293 cells. These data are consistent with a study that showed that it was the LIM domain and the first nebulin repeat that confer F-actin binding and that this F-actin-binding activity was essential for targeting of *lasp-2* to filopodial actin bundles (Nakagawa *et al.*, 2009).

In addition, even though GFP-*lasp-2* 161–273 would be predicted to have the ability to bind to vinculin (because it contains the SH3 domain of *lasp-2*), endogenous vinculin protein localization was not detectably altered in focal adhesions when these fragments were expressed (Figure 6).

Knockdown of *Lasp-2* increases cell spreading rates

Lasp-2 is localized to focal adhesions and binds to several key focal adhesion components. To investigate whether the loss of *lasp-2* has functional consequences in cell adhesion and dynamics, such as

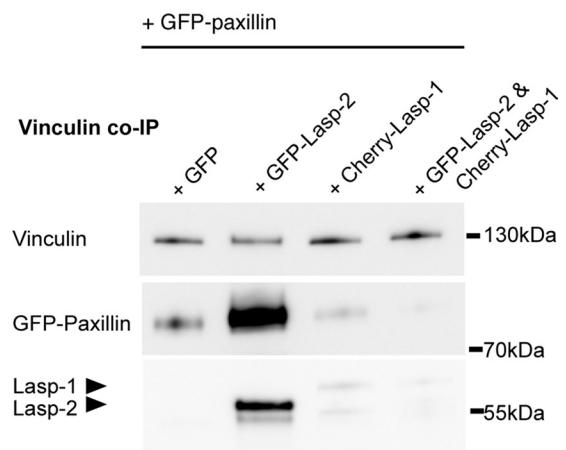


FIGURE 5: The interaction of vinculin and paxillin is enhanced in the presence of *lasp-2* and diminished in the presence of *lasp-1*. Vinculin and paxillin are known binding partners, and the presence of GFP-*lasp-2* enhances the amount of paxillin protein that is coimmunoprecipitated with vinculin in HEK 293 lysates when compared with controls. Endogenous vinculin was immunoprecipitated from cell lysates expressing GFP-paxillin and GFP, GFP-*lasp-2*, Cherry-*lasp-1*, or GFP-*lasp-2* and Cherry-*lasp-1* together. GFP-paxillin is more robustly coimmunoprecipitated in lysates with GFP-*lasp-2*. This enhancement is not detectable when *lasp-2* is lost from the complex as a result of Cherry-*lasp-1* expression.

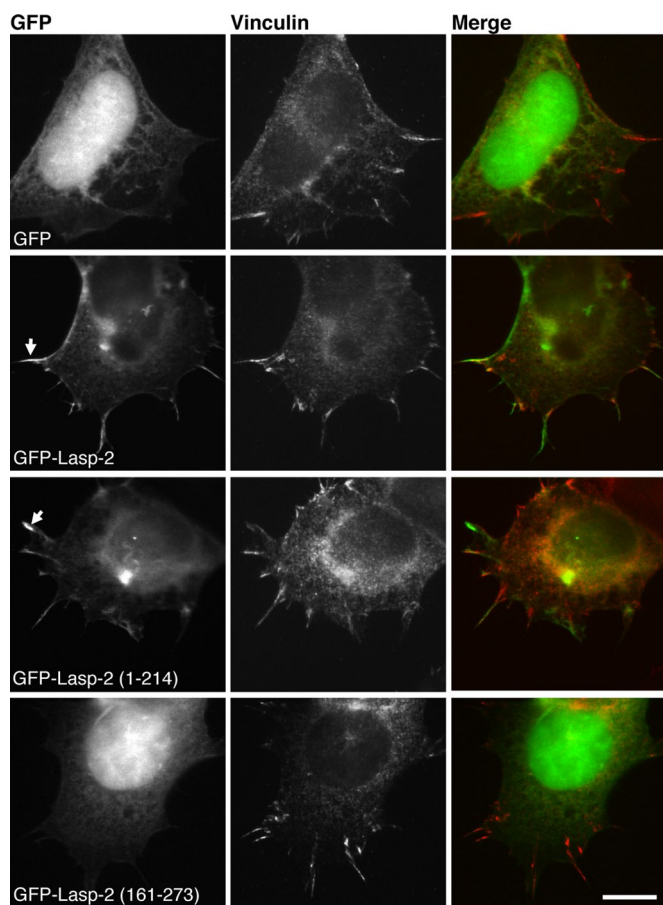


FIGURE 6: The LIM domain and nebulin repeats are necessary for localizing *lasp-2* in HEK 293 cells. GFP–*Lasp-2* and GFP–*Lasp-2* 1–214 assemble in similar patterns at focal adhesions (arrows) in HEK 293 cells, whereas GFP–*Lasp-2* 161–273 and GFP are predominantly nuclear, with some diffuse cytoplasmic distribution. Staining for endogenous vinculin marks sites of adhesion. These results indicate that the linker–SH3 domain (161–273) of *lasp-2* is not necessary for its proper localization. Scale bar, 10 μ m.

the ability of cells to spread, we performed *lasp-2*–knockdown experiments using small interfering RNA (siRNA). Cell spreading was observed in HEK 293 cells with depleted levels of *lasp-2*. Briefly, cells were transfected with *lasp-2* siRNA or control scrambled siRNA; protein knockdown of *lasp-2* was verified using anti–*lasp-2* antibodies via Western blots (Figure 7A). At 72 h later, the cells were trypsinized and replated onto coverslips and allowed to spread for 30 min. The spread area was measured using Cell Profiler (Carpenter *et al.*, 2006). Reproducibly, the spread area in the *lasp-2*–knockdown cells was increased by ~15% when compared with control cells. Three different sequences of siRNA to human *lasp-2* were used, each yielding similar increases in cell spreading. One representative experiment out of three replicates for one of the siRNA sequences is shown (Figure 7B). Although the measured spread area was enhanced in the cells with reduced *lasp-2*, the cells had similar morphology and adhesion when compared with the control siRNA cells. All cells exhibited abundant filopodial outgrowths and similar patterns of actin filament organization. These data suggest that the loss of *lasp-2* leads to a functional change in the ability of the cell to spread without altering cell morphology or actin filament organization.

Overexpression of *Lasp-2* increases the migration rate but decreases the invasion of cancer cells

Cancer cell metastasis involves increased cell migration and dysregulation of normal adhesion components and signaling. Given that *lasp-2* is a component of focal adhesions with several key binding partners that are involved in cell migration, the role of *lasp-2* in cell migration was examined. Two different metastatic cell lines were used, SW620 and PC-3B1. Derived from lymph node cells from a colorectal cancer patient, SW620 cells are metastatic (Leibovitz *et al.*, 1976) and contain low levels of endogenous *lasp-2* (unpublished data). PC-3B1 cells are a highly metastatic version of PC-3 cells (Sroka *et al.*, 2009) and were derived from the bone metastasis of a prostate cancer patient (Kaighn *et al.*, 1979). To study the role of *lasp-2* in cell migration, we performed a wound-healing assay. GFP–*lasp-2* or GFP alone was expressed in SW620 or PC-3B1 cells. The cells were scraped and monitored for wound closure. Both SW620 cells and PC-3B1 cells expressing GFP–*lasp-2* closed significantly faster (~3- and 1.4-fold, respectively) than cells expressing GFP alone (Figure 8A). Our *in vitro* binding data indicate that the presence of *lasp-2* enhances the interaction of vinculin and paxillin. Functionally, the excess *lasp-2* could be acting in a dominant-negative capacity by effectively sequestering the complex of vinculin and paxillin. This could reduce the stability of the focal adhesions, leading to increased migration.

In addition to the ability to migrate, metastatic cells must also be able to invade tissue barriers. To examine whether *lasp-2* also had an effect on cell invasion, we performed invasion chamber assays. SW620 or PC-3B1 cells expressing either GFP or GFP–*lasp-2* were plated onto Matrigel-coated invasion chambers and allowed to invade. Surprisingly, cells expressing GFP–*lasp-2* invaded the chamber an average of 11-fold less in SW620 cells and 4-fold less in PC-3B1 cells than in control cells expressing GFP alone (Figure 8B).

To determine whether the loss of *lasp-2* had an opposite effect on invasion compared with *lasp-2* overexpression, we assessed cells with *lasp-2* knockdown via siRNA (using two different siRNA sequences) for their ability to invade. PC-3 cells (Kaighn *et al.*, 1979)—prostate cancer cells (from which PC-B1 cells are derived)—were used because they express higher levels of endogenous *lasp-2* than the related PC-3B1 cells. PC-3 cells with *lasp-2* protein knocked down invaded the Matrigel-coated invasion chambers an average of approximately twofold more than control cells treated with a scrambled siRNA (Figure 8C). Similar results were found using both siRNA sequences. Collectively, these experiments reveal that *lasp-2* enhances cancer cell migration but reduces cell invasion.

DISCUSSION

To discover insights into the functional role of *lasp-2*, we identified additional binding partners. Our data show that *lasp-2* directly interacts with two well-described focal adhesion components—vinculin and paxillin—through its SH3 domain. *Lasp-2* enhances the binding of vinculin and paxillin with each other, whereas the presence of *lasp-1* reduces this effect. Although the SH3 domain contains the binding sites for *Lasp-2*'s focal adhesion–binding partners, the LIM and nebulin repeats containing its actin-binding domains are clearly required for targeting *lasp-2* to focal adhesions. Altering the levels of *lasp-2* revealed a role for this protein in cell spreading, migration, and invasion. Taken together, these results indicate that *lasp-2* is an important component of cell adhesion complexes and has functional roles in cell motility.

The binding site on *lasp-2* for vinculin and paxillin is the SH3 domain, which is also the mapped binding site for zyxin on *lasp-2* (Li *et al.*, 2004). Because SH3 domains often interact with

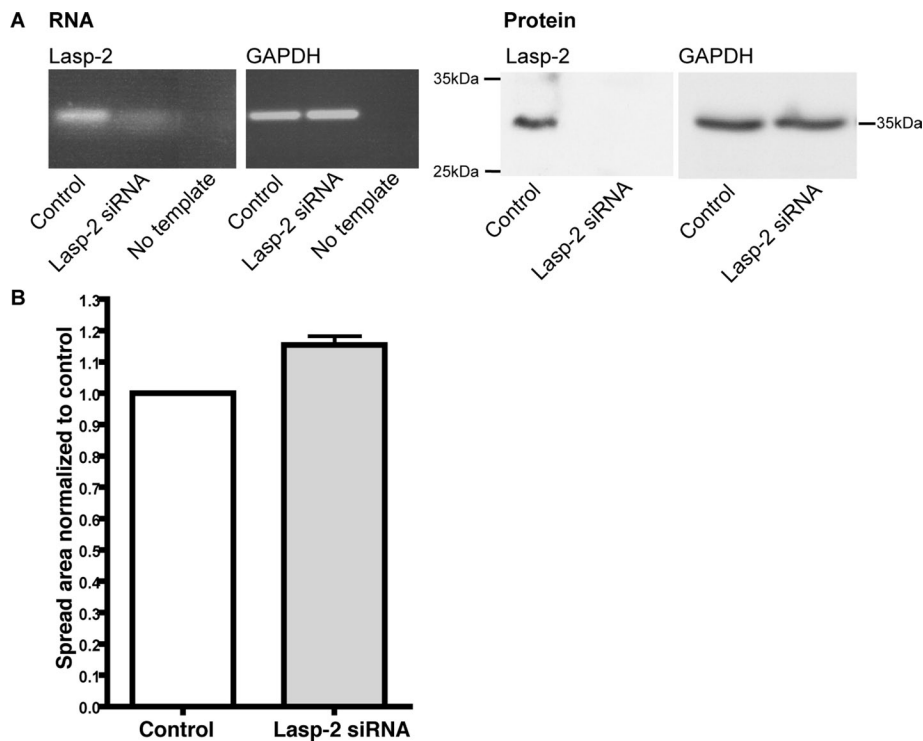


FIGURE 7: The knockdown of *lasp-2* increases cell spreading rates. (A) siRNA to human *lasp-2* was used to reduce *lasp-2* RNA and protein levels in HEK 293 cells. RT-PCR shows that *lasp-2* transcript is greatly reduced with *lasp-2* siRNA. *Lasp-2* protein levels are also significantly reduced with *lasp-2* siRNA treatment. (B) In cell-spreading assays, the spread area of *lasp-2* siRNA-treated cells was ~15% increased in comparison to controls.

multiple proteins, it is likely that there are additional mechanisms used by the cell to dictate when and how frequently *lasp-2* interacts with each of its binding partners. In fact, because the SH3 domain is a highly conserved protein interaction motif found in hundreds of mammalian proteins and is responsible for governing the assembly of protein complexes and intracellular signaling, there is much discussion on how specificity is achieved in pairwise SH3–ligand interactions (e.g., Ladbury and Arold, 2000; Li, 2005). It has been proposed that compartmentalization of potential interaction partners is one way to confer specificity (Mayer, 2001). To this end, an elegant study by Kanchanawong *et al.* (2010) using superresolution microscopy showed that focal adhesions have partially overlapping strata of protein interacting zones (i.e., integrin signaling layer, force transduction layer, and an actin regulatory layer). Although these strata are not strict compartments, the location of *lasp-2* either in or between one or two of these layers could be one of the mechanisms dictating the duration and frequency of the interactions with each of its binding partners.

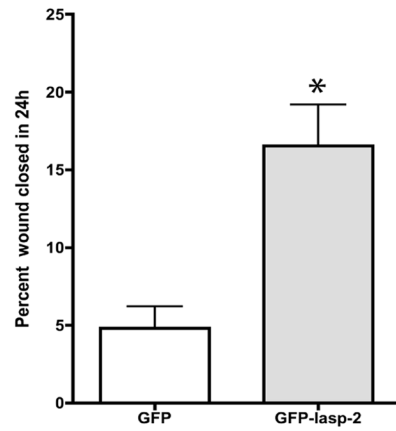
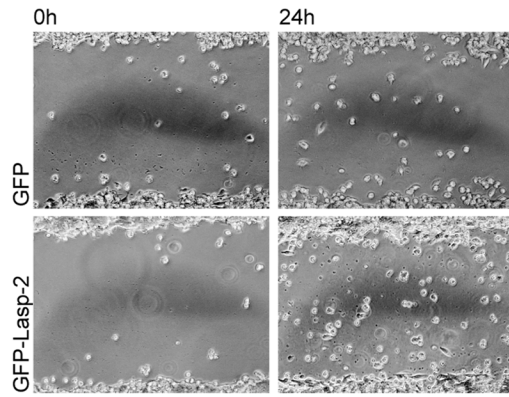
Whereas *lasp-2* interacts with vinculin and paxillin in cells, the presence of overexpressed *lasp-1* disrupts this interaction without itself appearing to be a major component of the complex. A potential explanation for this is that *lasp-1* may physically interact with *lasp-2*, preventing *lasp-2* from binding to paxillin or vinculin. In fact, our data show that *lasp-2* does interact with *lasp-1* with an *in vitro* K_D of 15 nM. The antagonistic roles of *lasp-1* and *lasp-2* would be predicted to provide yet another layer of regulation for adhesion structures. The differences in binding partners between *lasp-2* and *lasp-1* would also be predicted to represent another level of regulation of the two proteins.

Vinculin and paxillin are known binding partners (Turner *et al.*, 1990). It has been suggested that the *direct* association of vinculin-tail and paxillin in cells is weak and may require an indirect association through another protein (Humphries *et al.*, 2007). Of interest, the interaction of vinculin and paxillin was significantly enhanced in the presence of *lasp-2*. As such, our data suggest that *lasp-2* may, in fact, represent the predicted missing protein that enhances the association of vinculin with paxillin. Consistent with this idea is that the binding site for paxillin on vinculin is located within the vinculin-tail (amino acids 979–1028; Wood *et al.*, 1994) but is separate from the proline-rich region, the likely binding site for *lasp-2* (through its SH3 domain). Therefore it would be possible for vinculin to be bound to both paxillin and *lasp-2* at the same time. Perhaps *lasp-2* helps to facilitate the interaction of vinculin and paxillin by physically keeping the proteins near one another and/or recruiting yet another, unidentified binding protein. Of note, a complication to this possibility is that it would be unlikely for the SH3 domain of *lasp-2* to be bound to vinculin and paxillin simultaneously. However, because *lasp-2* and vinculin share actin as a binding partner, actin filaments could be involved in bringing different molecules of *lasp-2* bound to vinculin and paxillin together in a complex. It is also conceivable that *lasp-2* forms dimers (likely through its LIM domain, since this domain is commonly used for dimerization; Feuerstein *et al.*, 1994): one member of the dimer could bind vinculin, and the other could bind paxillin.

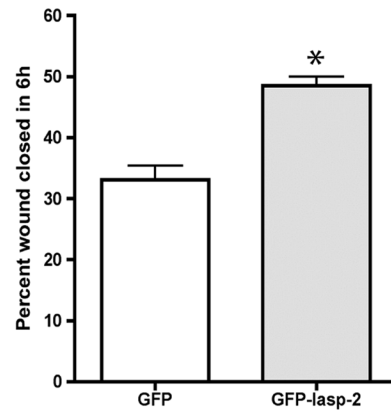
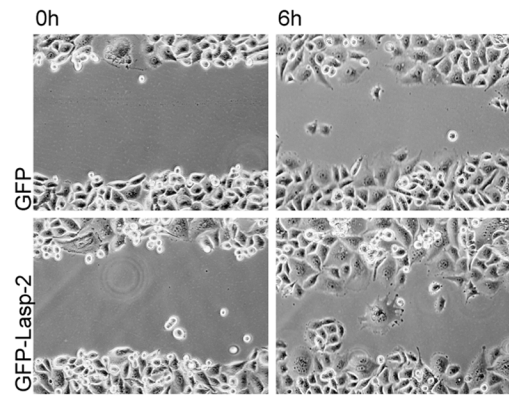
In HEK 293 cells *lasp-2* does not require its SH3 or linker–SH3 domain for proper localization but instead requires the LIM domain and nebulin repeats, suggesting that it is the actin-binding ability of *lasp-2* that first localizes the protein to focal adhesions and the cortical actin cytoskeleton. This idea is consistent with work by Nakagawa *et al.* (2009), which reported that the LIM and first nebulin repeat allow for proper localization of *lasp-2* in neuroblastoma cells (NG-108), and also by (Li *et al.*, 2004), which showed that the *lasp-2* SH3 domain alone was primarily localized to the nucleus of HeLa cells and *not* focal adhesions. In contrast, several studies in fibroblast cell lines concluded that it is the linker and SH3 domain of *lasp-2* that are necessary for the assembly of *lasp-2* to focal adhesions (Panaviene and Moncman, 2007; Nakagawa *et al.*, 2009). Of interest, it is also the linker–SH3 domain that is mainly responsible for targeting it to the Z-disks of mature cardiomyocytes, although it should be noted that a fragment of *lasp-2* that contained the LIM domain, nebulin repeats, and linker was also able to weakly target to the Z-disk (Zieseniss *et al.*, 2008). The present study suggests that HEK 293 cells display a cytoskeletal and cell adhesion organization that differ from common fibroblast lines. Thus it appears that *lasp-2* is a multifunctional protein whose domains play different roles depending on the constituents of the cytoskeletal assemblies with which it associates.

Knockdown of *lasp-2* in HEK 293 cells resulted in a significant increase (~15%) in cell spreading rate. The enhanced cell spreading with loss of *lasp-2* may be a function of a change in the dynamics of

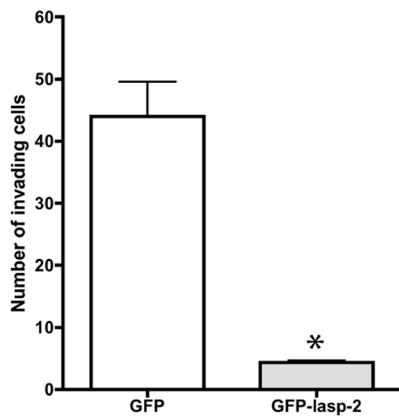
A SW620 cells



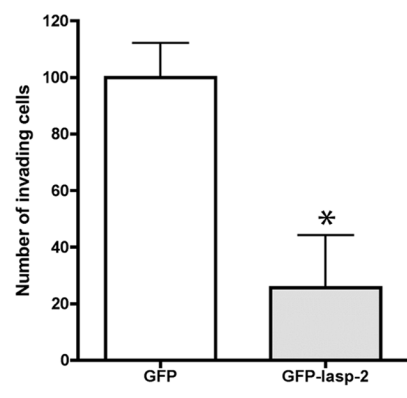
PC-3B1 cells



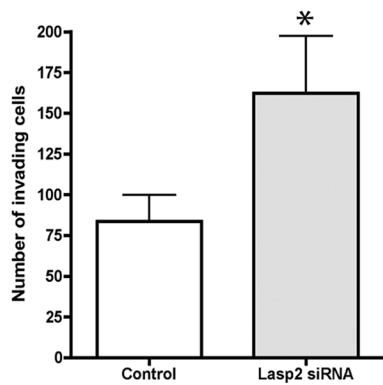
B SW620 cells



PC-3B1 cells



C PC-3 cells



key focal adhesion components. Focal adhesions are in a constant state of assembly, stabilization, and turnover, and cell spreading represents a state in which focal adhesion formation exceeds turnover (for review see Nagano *et al.*, 2012). Because a number of focal adhesion components are *lasp-2* binding partners (vinculin, paxillin, and zyxin), perhaps the loss of *lasp-2* alters the dynamics of one or more of these proteins and leads to a functional change in cell spreading rates.

A process that is intimately involved in cell adhesion dynamics, cell migration, and invasion is metastasis. The exact mechanisms that lead to metastasis are not fully known, and proteins related to migration and the actin cytoskeleton are often targets of study. Indeed, overexpression of *lasp-2* enhanced cell migration but reduced invasion in SW620 colorectal cancer cells and PC-3B1 prostate cancer cells. A recent study that knocked down the *lasp-2* related protein *lasp-1* in SW620 cells found that both cell migration and invasion were reduced (Zhao *et al.*, 2010); this result suggests that alterations of *lasp-1* protein levels affect cell migration in a similar manner to *lasp-2*, but the invasion potential differs between the two proteins, as *lasp-2* did not facilitate cell invasion. Cell invasion involves a complex of different factors, including migration, but also adhesion and proteolysis of extracellular matrix components (for reviews see Friedl and Wolf, 2003; Yamaguchi and Condeelis, 2007). Thus, although the role of *lasp-2* and *lasp-1* in cell migration is perhaps a shared function, the process of cell invasion highlights key differences between *lasp-1* and *lasp-2*, and interplay in the amount of *lasp-1* and *lasp-2* in cells could be a regulatory mechanism for cell migration and invasion. For instance, for a cancer cell to become metastatic, enhanced protein levels of *lasp-2* would be beneficial for migration but *lasp-2* protein levels would need to be down-regulated to penetrate tissue barriers.

Of interest, *lasp-2* overexpression in SW620 cells and PC-3B1 cells reveals invasion and migration dynamics more similar to that in cells with decreased vinculin expression. Vinculin-null cells migrate more rapidly but have reduced invasion (Goldmann *et al.*, 1995; Mierke *et al.*, 2010), similar to *lasp-2*-overexpressing cells. The mechanisms explaining this include that the lack of vinculin destabilizes focal adhesion structures, leading to increased migration, as well as reducing contractile force generation (since it is a mechano-regulating protein; Mierke *et al.*, 2008), and this interferes with invasion. It is possible that the overexpression of *lasp-2* in metastatic cells could effectively bind up a significant amount of endogenous vinculin, thus inhibiting vinculin from interacting with its many other binding partners and performing some of its cellular functions, mimicking a vinculin knockdown.

We conclude that *lasp-2* is an important member of focal adhesions. Through interactions with its binding partners, *lasp-2* clearly has roles in focal adhesion composition, maintenance, and signaling. *Lasp-2* also can facilitate the interaction of several key focal adhesion components making it a potentially important scaffolding protein in cell adhesion. Our data are also consistent with *Lasp-2*

having potentially significant roles in cell motility, with dual functions for migration and invasion.

MATERIALS AND METHODS

Cell culture and transfection

HEK 293 and SW620 cells were maintained in high-glucose DMEM (Invitrogen, Carlsbad, CA) supplemented with 10% fetal bovine serum (FBS), 4 mM L-glutamine, 1 mM sodium pyruvate, 0.1 mM MEM nonessential amino acids, and 1% penicillin–streptomycin. PC-3B1 and PC-3 prostate cancer cells were a generous gift from Anne Cress (University of Arizona, Tucson, AZ). These cells were maintained in Iscove's modified Dulbecco's medium (Invitrogen) supplemented with 10% FBS and 1% penicillin–streptomycin. Cells were plated into 35-mm tissue culture dishes at a density of 1×10^5 cells/dish. For imaging experiments, the cells were plated on 12-mm-diameter glass coverslips. Transfections of GFP-tagged constructs were performed with Effectene transfection reagent (Qiagen, Valencia, CA) according to the manufacturer's specifications. The culture medium was changed 24 h after transfection.

Construct preparation

For cloning primer design of full-length *lasp-2* and *lasp-2* truncations see Zieseniss *et al.* (2008). Briefly, constructs were cloned into pEGFP-C2 (Clontech, Mountain View, CA) using 5' *EcoRI* and 3' *XhoI* restriction sites. Full-length *lasp-1* was amplified from mouse cDNA and cloned into mCherry-C2 (Clontech) using 5' *EcoRI* and 3' *XhoI* restriction sites (forward primer 5'-TAGAATTCATGAACCCTAACTGTGCC-3' and reverse primer 5'-ATGTCGACTCAGATGGCCTCCACGTA-3').

Immunofluorescence microscopy

HEK 293 cells were fixed in 3% formaldehyde for 15 min, permeabilized with 0.2% Triton X-100/phosphate-buffered saline (PBS), and blocked with 2% bovine serum albumin (BSA)/1% normal donkey serum/PBS. Cells were incubated with monoclonal anti-vinculin antibodies (1:2000; Sigma-Aldrich, St. Louis, MO) or monoclonal anti-paxillin antibodies (1:100; BD Biosciences, San Jose, CA), followed by Texas red–conjugated donkey anti-mouse immunoglobulin G (IgG; 1:600; Jackson ImmunoResearch Laboratories, West Grove, PA). For spreading assays, cells were stained with Texas red–phalloidin (1:100; Invitrogen) to mark F-actin. Coverslips were mounted on slides using Aqua PolyMount (Polysciences, Warrington, PA) and analyzed with an inverted fluorescence microscope (Carl Zeiss, Oberkochen, Germany) using a 100x/numerical aperture 1.25 objective, and micrographs were collected as digital images (OrcaER; Hamamatsu, Hamamatsu City, Japan) using OpenLab software (Improvision, PerkinElmer, Waltham, MA). Images were processed using Photoshop (Adobe, San Jose, CA).

Yeast two-hybrid assays

Full-length *lasp-2* was cloned into the yeast bait vector pGBKT7 (Clontech) downstream of the DNA-binding domain of GAL4.

FIGURE 8: The overexpression of *lasp-2* in SW620 and PC-3B1 cells increases cell migration rates but reduces cell invasion. (A) SW620 cells, derived from metastatic colorectal cancer, and PC-3B1 cells, derived from metastatic prostate cancer, migrated at a faster rate when GFP–*lasp-2* is expressed. There was a threefold increase in the wound-healing rate in cells expressing GFP–*lasp-2* in the SW620 cells. There was a 1.4-fold increase in the wound-healing rate in cells expressing GFP–*lasp-2* in the PC-3B1 cells. * $p < 0.05$. (B) Cell invasion is reduced in cells expressing GFP–*lasp-2*. GFP–*lasp-2*-expressing cells invaded the chamber an average of 11-fold less than control cells in SW620 cells and invaded the chamber an average of fourfold less than control cells in PC-3B1 cells. * $p < 0.005$. (C) Loss of *lasp-2* protein leads to an increase in cell invasion. Two different siRNA sequences to human *lasp-2* were used to reduce *lasp-2* protein levels in PC-3 cells. Cells with *lasp-2* protein knocked down invaded the chamber approximately twofold more than controls. Data from one of the siRNA sequences are shown. * $p < 0.05$.

Vinculin (full-length and head and tail regions), paxillin, and *lasp-1* were cloned into the yeast prey vector pGADT7 (Clontech) downstream of the transactivation domain of GAL4. *Lasp-2* bait was cotransformed into yeast strain AH109 with the vinculin, paxillin, or *lasp-1* prey constructs using the Yeastmaker Yeast Transformation Kit (Clontech) according to the manufacturer's specifications. Selection for positive interactions, and therefore activation of the *HIS3* and *ADE2*, was carried out on agar plates lacking tryptophan, leucine, histidine, and adenine. All constructs were determined not to be toxic to the yeast or to activate the reporter genes independently of a positive interaction (autoactivation).

Protein expression and purification

Full-length *lasp-2* and full-length *lasp-1* were prepared as GST-fusion proteins (in pGEX-4T; Amersham Biosciences/GE Healthcare, Waukesha, WI) in *Escherichia coli* cells (BL21DE) and purified using glutathione-Sepharose 4B (GE Healthcare) according to the manufacturer's specifications. Recombinant GST-*lasp-2* and GST-*lasp-1* were dialyzed against 20 mM NaPO₄ and 100 mM KCl, pH 7.2, flash frozen, and stored at -80°C until use. *Lasp-2* (full-length), vinculin-tail (amino acids 840–1066), and paxillin (full-length) were prepared as His-fusion proteins (in pET28a; Novagen/EMD Millipore, Billerica, MA) in BL21DE cells using nickel-nitriloacetic acid agarose (Qiagen, Valencia, CA) according to the manufacturer's specifications. Recombinant His-vinculin-tail was dialyzed against 20 mM 4-(2-hydroxyethyl)-1-piperazineethanesulfonic acid (HEPES), 80 mM KCl, and 2 mM MgCl₂, pH 7.4. Recombinant His-paxillin was dialyzed against PBS, pH 7.4. Both proteins were flash frozen and stored at -80°C until use. His peptide used as a negative control was purchased from Abcam (Cambridge, United Kingdom).

Solid-phase binding assays

ELISAs were used to confirm the interaction of *lasp-2* with paxillin, *lasp-2* with vinculin, and *lasp-2* with *lasp-1*. For the interaction with vinculin, microtiter plates were coated with 10 pmol of His-vinculin-tail or His-peptide alone. Wells were washed with 0.1% Tween 20 in binding buffer (20 mM HEPES, pH 7.4, 120 mM NaCl, 80 mM KCl, 2 mM MgCl₂) and blocked with 2% BSA in binding buffer for 1 h at room temperature. Increasing amounts of His-tagged *lasp-2* in 1% BSA/binding buffer (0.1–25 pmol) were added to the wells and incubated for 1.5 h at room temperature. Bound *lasp-2* was detected with anti-*lasp-2* antibodies (1 µg/ml), followed by a goat anti-mouse alkaline phosphatase-conjugated IgG (Jackson ImmunoResearch Laboratories). For the interaction with paxillin, microtiter plates were coated with 10 pmol of GST-*lasp-2* (or GST alone). Increasing amounts of His-tagged paxillin (0.1–25 pmol) were added to the wells, which were incubated for 1.5 h at room temperature. Bound paxillin was detected with anti-paxillin antibodies (0.1 µg/ml; BD BioSciences), followed by a goat anti-mouse alkaline phosphatase-conjugated IgG (Jackson ImmunoResearch Laboratories). For the interaction with *lasp-1*, microtiter plates were coated with 10 pmol of His-*lasp-2* or his peptide alone. Increasing amounts of GST-*lasp-1* were added to the wells, which were incubated for 1.5 h at room temperature. Bound GST-*lasp-1* was detected using an anti-GST antibody (0.2 µg/ml; Sigma-Aldrich), followed by a goat anti-mouse alkaline phosphatase-conjugated IgG (Jackson ImmunoResearch Laboratories). For all ELISAs, enzyme activity was measured using 4-nitrophenyl phosphate disodium salt hexahydrate (Sigma-Aldrich) as a substrate at 405 nm using a microplate reader (Tecan Group, Mannedorf, Switzerland). Prism (GraphPad, San Diego, CA) was used for analysis and presentation of the data.

Coimmunoprecipitation experiments

HEK 293 cells were plated on 10-cm tissue culture dishes transfected with plasmids encoding GFP, GFP-*lasp-2*, Cherry-*lasp-1*, or Cherry-*lasp-1* and GFP-*lasp-2*. At 48 h after transfection, lysate was harvested in ice-cold immunoprecipitation buffer (137 mM NaCl, 1% NP-40, 20 mM Tris-HCl, pH 8.0, 2 mM EDTA, 10% glycerol) with protease inhibitors. After sonication and centrifugation for 15 min at 16,000 × g to remove insoluble debris, total protein levels were measured using a bicinchoninic acid assay (ThermoFisher Scientific, Waltham, MA). We used 1.5 mg of lysate per immunoprecipitation. The lysate was precleared with 50 µl of protein A/G agarose beads (Santa Cruz Biotechnology, Santa Cruz, CA) for 2 h and then combined with 2 µg of either anti-vinculin (Sigma-Aldrich) or anti-paxillin antibodies (BD Biosciences) overnight. We then added 100 µl of protein A/G beads for an additional 4 h. The beads/antibody/lysate was washed four times with immunoprecipitation buffer and the sample prepared for Western blot analysis. Each coimmunoprecipitation was repeated at least three times, and a representative experiment is shown.

Generation of an anti-*Lasp-2* monoclonal antibody

To raise an antibody that is specific to *lasp-2* and does not recognize *lasp-1* and nebulette, we generated antibodies using a recombinant mouse/chicken (identical amino acid sequence) *lasp-2* fragment containing amino acids 1–119, conjugated to KLH (Invitrogen) as an antigen. Amino acids 1–119 represent the four unique exons in *lasp-2* that are not found in nebulette. Monoclonal antibodies were generated by BSBS Antibody Facility (Braunschweig, Germany). Clones were screened for reactivity to the antigen by ELISA. Positive clones were screened by Western blot analysis for specificity to *lasp-2* protein but not to *lasp-1*.

RT-PCR

Transcript levels of *lasp-2* were evaluated by PCR. Total RNA was extracted from cells with TRIzol reagent (Invitrogen) according to the manufacturer's instructions. RNA concentration was determined using a NanoDrop Spectrophotometer (ThermoFisher Scientific). cDNA was synthesized from 1 µg of total RNA using M-MLV reverse transcriptase (Invitrogen). This cDNA was used to assess transcript levels of genes with endpoint PCR. Primers used included human *lasp-2* (forward, 5'-CATTCCCAAGGCTATGGCTA-3'; reverse, 5'-ATCGTACATGGCTCGGTAGG-3') and human glyceraldehyde-3-phosphate dehydrogenase (GAPDH; forward, 5'-GAAGGTGAAGGTCGGAGTC-3'; reverse, 5'-GAAGATGGTATGGGATTC-3'). All primer sets were intron spanning. GoTaq (Promega, Madison, WI) was used for endpoint PCR to amplify *lasp-2* cDNA using 28 cycles.

Adenovirus preparation

A replication-defective adenovirus (Adv) expressing GFP or GFP-*Lasp-2* was constructed using the AdEasy Adenoviral Vector System from Stratagene (La Jolla, CA). Briefly, GFP or GFP-*Lasp-2* cDNA was subcloned into pShuttle-CMV plasmid and linearized according to the manufacturer's instructions before transformation of BJ5183 cells containing the pAdEasy-1 vector. After homologous recombination, the purified pAdEasy-1 vector containing GFP or GFP-*Lasp-2* was then transfected into HEK 293 cells for Adv propagation. In each experiment, a replication-defective Adv expressing GFP was used to control for nonspecific effects of Adv infection. All Adv were propagated in HEK 293 cells and purified by CsCl gradient centrifugation. The multiplicity of viral infection (MOI) was determined by viral dilution assay in HEK 293 cells grown in 96-well clusters. At a MOI of 5–10, >95% of the cells were infected, as determined by GFP-positive cells,

and there were no cytotoxic effects of Adv infection during the 24 h after Adv infection.

Western blot analysis

Whole-cell lysates from HEK 293 cells were prepared in SDS sample buffer, run on 8 or 10% SDS-PAGE, and transferred onto nitrocellulose membranes (Whatman, Kent, United Kingdom). Membranes were blocked in 2% BSA/PBS for 1 h at room temperature and incubated with primary antibodies to vinculin (1:10,000; Invitrogen), paxillin (1:2000; BD Biosciences), zyxin (1:1000; Invitrogen), *lasp-1* (1:2000; Chemicon/EMD Millipore), *lasp-2* (0.5 µg/ml; generated in this study; see earlier description), and GAPDH (1:40,000; Ambion/Life Technologies, Carlsbad, CA) for 1–2 h at room temperature. Blots were then incubated with horseradish peroxidase-conjugated secondary antibodies (1:10,000; Jackson ImmunoResearch) for 1 h, followed by chemiluminescence detection using West Pico substrate or West Femto (ThermoFisher Scientific) and visualized with either film or using a G:Box Chemi system (Syngene, Frederick, MD). Protein loading was assessed by GAPDH (loading control) and Coomassie blue staining of proteins in the gel. Protein level changes between experimental and control groups were quantified using ImageJ (National Institutes of Health, Bethesda, MA).

siRNA transfection

Three predesigned siRNA targeted specifically to *lasp-2* were obtained from Invitrogen: 1) sense, 5'-CAGCGAUGCUGC-CUAUAAAtt-3', and antisense, 5'-UUUAUAGGCAGCAUCGCU-Gac-3'; 2) sense, 5'-CAAUGCAGCAUUCACCAAAtt-3', and antisense, 5'-UUUGGUGAAUGCUGCAUUGac-3'; and 3) sense, 5'-CCCGGAGCCUAUCAGCAAAtt-3', and antisense, 5'-UUU-GCUGAUAGGCCUCCGGGac-3'. HEK 293 cells were maintained in complete media without antibiotics at ~60% confluence and then transfected with *lasp-2* siRNA using Lipofectamine RNAiMAX (Invitrogen) according to manufacturer's instructions and transfected a second time after 4 8h. Cells were analyzed 72 h after transfection. *Lasp-2* protein knockdown was monitored by Western blot analysis and RT-PCR.

Cell-spreading assay

HEK 293 cells were transfected with siRNA or control scrambled siRNA and cultured for 72 h. Cells were trypsinized and replated onto coverslips coated with collagen (Invitrogen) and allowed to spread for 30 min. The cells were then fixed with 3% formaldehyde and stained with Texas red-phalloidin (1:100; Invitrogen) to mark F-actin. The cells were imaged, and the spread area of each cell was calculated using Cell Profiler (Carpenter *et al.*, 2006). Three different siRNA sequences were used to knock down *lasp-2*, and similar results were obtained.

Wound-healing assays

SW620 or PC-B1 cells were transfected or infected with either GFP or GFP-*lasp-2* plasmids. At 48 h after transfection, a confluent monolayer of cells formed. Cells were serum starved overnight, and wounds were made with a pipette tip. Cells were imaged at wounding, and then the identical cells was imaged again at 24 and 48 h for SW620 cells and 6 and 12 h for PC-B1 cells (the wound closure rates varied for each cell type). The percentage of the wound closure area was evaluated using ImageJ.

Invasion chamber assays

In some experiments, SW620 or PC-3B1 cells were infected with either GFP or GFP-*lasp-2* plasmids. In other experiments, PC-3 cells

were transfected twice (with an interval of 48 h) with human *lasp-2*-specific siRNA or control scrambled siRNA. At 48 h after infection with plasmids or 72 h after transfection with siRNA, cells were trypsinized and replated into the top chamber of BD Biocoat Matrigel-coated invasion chambers with 8.0-µm pore sizes (BD Biosciences) at a density of 2.5×10^4 cells/0.5 ml in serum-free media. Complete medium was added to the bottom of the chamber. Cells were allowed to invade through the membrane for 22 h. Cells that did not invade through the membrane were scraped off according to manufacturer's instructions. For overexpression studies, the total number of infected cells that had migrated through the membrane was counted using a fluorescence microscope using GFP fluorescence to mark the cell, and each experiment was done in technical triplicate. For knockdown studies, the cells that had invaded through the chamber were fixed and stained with crystal violet solution to mark the cells. The total number of invaded cells was quantified, and each experiment was done in technical triplicate. Two different siRNA sequences were used, with similar results obtained.

Statistics

A paired Student's *t* test was used to test significance in the cell-spreading and migration/invasion experiments.

ACKNOWLEDGMENTS

We thank Anke Ziesenis for initiating these studies and preparing the GFP-*lasp-2* constructs, Cathleen Cover for purification of *lasp-2* protein, Yasuko Ono and Christine Henderson for consultation and assistance on yeast two-hybrid assays, Chinedu Nworu for assistance with Cell Profiler, and Anne Cress for providing the PC-3B cell line. This work was supported by an American Heart Association Predoctoral Fellowship (10PRE3780013) and a National Heart, Lung, and Blood Institute Training Grant (T32 HL07249) to K.B., the Undergraduate Biology Research Program (HHMI52005889) to C.M.J.W., and National Institutes of Health Grants HL083146 and HL108625 to C.C.G.

REFERENCES

- Beckerle MC (1997). Zyxin: zinc fingers at sites of cell adhesion. *Bioessays* 19, 949–957.
- Carpenter AE *et al.* (2006). CellProfiler: image analysis software for identifying and quantifying cell phenotypes. *Genome Biol* 7, R100.
- Chew CS, Chen X, Parente JAJr, Tarrer S, Okamoto C, Qin HY (2002). *Lasp-1* binds to non-muscle F-actin in vitro and is localized within multiple sites of dynamic actin assembly in vivo. *J Cell Sci* 115, 4787–4799.
- Crawford AW, Beckerle MC (1991). Purification and characterization of zyxin, an 82,000-dalton component of adherens junctions. *J Biol Chem* 266, 5847–5853.
- Deng XA, Norris A, Panavieni Z, Moncman CL (2008). Ectopic expression of LIM-nebulette (LASP2) reveals roles in cell migration and spreading. *Cell Motil Cytoskeleton* 65, 827–840.
- Deramandt TB, Dujardin D, Hamadi A, Noulet F, Kolli K, De Mey J, Takeda K, Ronde P (2011). FAK phosphorylation at Tyr-925 regulates cross-talk between focal adhesion turnover and cell protrusion. *Mol Biol Cell* 22, 964–975.
- Feuerstein R, Wang X, Song D, Cooke NE, Liebhaber SA (1994). The LIM/double zinc-finger motif functions as a protein dimerization domain. *Proc Natl Acad Sci USA* 91, 10655–10659.
- Friedl P, Wolf K (2003). Tumour-cell invasion and migration: diversity and escape mechanisms. *Nat Rev Cancer* 3, 362–374.
- Gardel ML, Schneider IC, Aratyn-Schaus Y, Waterman CM (2010). Mechanical integration of actin and adhesion dynamics in cell migration. *Annu Rev Cell Dev Biol* 26, 315–333.
- Goldmann WH, Schindl M, Cardozo TJ, Ezzell RM (1995). Motility of vinculin-deficient F9 embryonic carcinoma cells analyzed by video, laser confocal, and reflection interference contrast microscopy. *Exp Cell Res* 221, 311–319.
- Grunewald TG, Kammerer U, Schulze E, Schindler D, Honig A, Zimmer M, Butt E (2006). Silencing of LASP-1 influences zyxin localization, inhibits

- proliferation and reduces migration in breast cancer cells. *Exp Cell Res* 312, 974–982.
- Grunewald TG, Kammerer U, Winkler C, Schindler D, Sickmann A, Honig A, Butt E (2007). Overexpression of LASP-1 mediates migration and proliferation of human ovarian cancer cells and influences zyxin localisation. *Br J Cancer* 96, 296–305.
- Hervy M, Hoffman L, Beckerle MC (2006). From the membrane to the nucleus and back again: bifunctional focal adhesion proteins. *Curr Opin Cell Biol* 18, 524–532.
- Hirata H, Tatsumi H, Sokabe M (2008). Mechanical forces facilitate actin polymerization at focal adhesions in a zyxin-dependent manner. *J Cell Sci* 121, 2795–2804.
- Humphries JD, Wang P, Streuli C, Geiger B, Humphries MJ, Ballestrem C (2007). Vinculin controls focal adhesion formation by direct interactions with talin and actin. *J Cell Biol* 179, 1043–1057.
- Kaighn ME, Narayan KS, Ohnuki Y, Lechner JF, Jones LW (1979). Establishment and characterization of a human prostatic carcinoma cell line (PC-3). *Invest Urol* 17, 16–23.
- Kanchanawong P, Shtengel G, Pasapera AM, Ramko EB, Davidson MW, Hess HF, Waterman CM (2010). Nanoscale architecture of integrin-based cell adhesions. *Nature* 468, 580–584.
- Katoh M (2003). Identification and characterization of LASP2 gene in silico. *Int J Mol Med* 12, 405–410.
- Labeit S, Gibson T, Lakey A, Leonard K, Zeviani M, Knight P, Wardale J, Trinick J (1991). Evidence that nebulin is a protein-ruler in muscle thin filaments. *FEBS Lett* 282, 313–316.
- Ladbury JE, Arold S (2000). Searching for specificity in SH domains. *Chem Biol* 7, R3–8.
- Le Clairche C, Carlier MF (2008). Regulation of actin assembly associated with protrusion and adhesion in cell migration. *Physiol Rev* 88, 489–513.
- Leibovitz A, Stinson JC, McCombs WB3rd, McCoy CE, Mazur KC, Mabry ND (1976). Classification of human colorectal adenocarcinoma cell lines. *Cancer Res* 36, 4562–4569.
- Li B, Zhuang L, Trueb B (2004). Zyxin interacts with the SH3 domains of the cytoskeletal proteins LIM-nebulette and Lasp-1. *J Biol Chem* 279, 20401–20410.
- Li SS (2005). Specificity and versatility of SH3 and other proline-recognition domains: structural basis and implications for cellular signal transduction. *Biochem J* 390, 641–653.
- Lin YH, Park ZY, Lin D, Brahmabhatt AA, Rio MC, Yates JR 3rd, Klemke RL (2004). Regulation of cell migration and survival by focal adhesion targeting of Lasp-1. *J Cell Biol* 165, 421–432.
- Lo SH (2006). Focal adhesions: what's new inside. *Dev Biol* 294, 280–291.
- Mayer BJ (2001). SH3 domains: complexity in moderation. *J Cell Sci* 114, 1253–1263.
- Mierke CT, Kollmannsberger P, Zitterbart DP, Diez G, Koch TM, Marg S, Ziegler WH, Goldmann WH, Fabry B (2010). Vinculin facilitates cell invasion into three-dimensional collagen matrices. *J Biol Chem* 285, 13121–13130.
- Mierke CT, Kollmannsberger P, Zitterbart DP, Smith J, Fabry B, Goldmann WH (2008). Mechano-coupling and regulation of contractility by the vinculin tail domain. *Biophys J* 94, 661–670.
- Moncman CL, Wang K (1995). Nebulette: a 107 kD nebulin-like protein in cardiac muscle. *Cell Motil Cytoskeleton* 32, 205–225.
- Nagano M, Hoshino D, Koshikawa N, Akizawa T, Seiki M (2012). Turnover of focal adhesions and cancer cell migration. *Int J Cell Biol* 2012, 310616.
- Nakagawa H, Suzuki H, Machida S, Suzuki J, Ohashi K, Jin M, Miyamoto S, Terasaki AG (2009). Contribution of the LIM domain and nebulin-repeats to the interaction of Lasp-2 with actin filaments and focal adhesions. *PLoS One* 4, e7530.
- Panaviene Z, Moncman CL (2007). Linker region of nebulin family members plays an important role in targeting these molecules to cellular structures. *Cell Tissue Res* 327, 353–369.
- Schreiber V, Moog-Lutz C, Regnier CH, Chenard MP, Boeuf H, Vonesch JL, Tomasetto C, Rio MC (1998). Lasp-1, a novel type of actin-binding protein accumulating in cell membrane extensions. *Mol Med* 4, 675–687.
- Smith MA, Blankman E, Gardel ML, Luettjohann L, Waterman CM, Beckerle MC (2010). A zyxin-mediated mechanism for actin stress fiber maintenance and repair. *Dev Cell* 19, 365–376.
- Sroka IC, Pond GD, Nagle RB, Porreca F, King T, Pestano G, Futscher BW, Gard JM, Riley J, Cress AE (2009). Human cell surface receptors as molecular imaging candidates for metastatic prostate cancer. *Open Prostate Cancer J* 2, 59–66.
- Terasaki AG, Suzuki H, Ando J, Matsuda Y, Ohashi K (2006). Chromosomal assignment of LASP1 and LASP2 genes and organization of the LASP2 gene in chicken. *Cytogenet Genome Res* 112, 141–147.
- Terasaki AG, Suzuki H, Nishioka T, Matsuzawa E, Katsuki M, Nakagawa H, Miyamoto S, Ohashi K (2004). A novel LIM and SH3 protein (lasp-2) highly expressing in chicken brain. *Biochem Biophys Res Commun* 313, 48–54.
- Tomasetto C, Moog-Lutz C, Regnier CH, Schreiber V, Basset P, Rio MC (1995). Lasp-1 (MLN 50) defines a new LIM protein subfamily characterized by the association of LIM and SH3 domains. *FEBS Lett* 373, 245–249.
- Turner CE, Glenney JR Jr, Burrige K (1990). Paxillin: a new vinculin-binding protein present in focal adhesions. *J Cell Biol* 111, 1059–1068.
- Wang Y, Gilmore TD (2003). Zyxin and paxillin proteins: focal adhesion plaque LIM domain proteins go nuclear. *Biochim Biophys Acta* 1593, 115–120.
- Wood CK, Turner CE, Jackson P, Critchley DR (1994). Characterisation of the paxillin-binding site and the C-terminal focal adhesion targeting sequence in vinculin. *J Cell Sci* 107 (Pt 2), 709–717.
- Wozniak MA, Modzelewska K, Kwong L, Keely PJ (2004). Focal adhesion regulation of cell behavior. *Biochim Biophys Acta* 1692, 103–119.
- Yamaguchi H, Condeelis J (2007). Regulation of the actin cytoskeleton in cancer cell migration and invasion. *Biochim Biophys Acta* 1773, 642–652.
- Yu H, Chen JK, Feng S, Dalgarno DC, Brauer AW, Schreiber SL (1994). Structural basis for the binding of proline-rich peptides to SH3 domains. *Cell* 76, 933–945.
- Zhang H, Chen X, Bollag WB, Bollag RJ, Sheehan DJ, Chew CS (2009). Lasp1 gene disruption is linked to enhanced cell migration and tumor formation. *Physiol Genomics* 38, 372–385.
- Zhao L *et al.* (2010). Promotion of colorectal cancer growth and metastasis by the LIM and SH3 domain protein 1. *Gut* 59, 1226–1235.
- Zieseniss A, Terasaki AG, Gregorio CC (2008). Lasp-2 expression, localization, and ligand interactions: a new Z-disc scaffolding protein. *Cell Motil Cytoskeleton* 65, 59–72.